Simulation study of the role of the ribosomal exit tunnel on protein folding

Changjun Chen, Ercheng Wang, Pengyu Liu, and Yi Xiao*

Biomolecular Physics and Modeling Group, Department of Physics, Huazhong University of Science and Technology, Wuhan 430074, Hubei, China

(Received 8 November 2011; revised manuscript received 14 January 2013; published 4 February 2013)

To investigate the role of the ribosomal exit tunnel on protein folding, we simulate the initial-stage folding behavior of the protein villin headpiece subdomain HP35 (PDB id: 1yrf) with and without prefolding in the exit tunnel by using an all-atom model and find that prefolding in the exit tunnel could effectively help the protein form native secondary structures. Furthermore, our results show that, after releasing from the exit tunnel, the prefolded chains may have a tendency to form more native contacts than those only in free space and this reduces the conformational space of sampling. Our results may provide an alternative way to explain the fast folding mechanism of proteins *in vivo*.

DOI: 10.1103/PhysRevE.87.022701 PACS number(s): 87.15.Cc, 87.15.ap

I. INTRODUCTION

Nascent peptide chains go through a long exit tunnel in the ribosome after they are synthesized at the peptidyl transferase center (PTC). The exit tunnel is cylinder-like and of about 100 Å length and 10–20 Å width [1]. The crossing speed of the peptide chains in it is about several amino acids per second, like their synthesizing speeds on PTC [2]. Therefore, the nascent peptide chain may start to fold within the exit tunnel [3]. However, the ribosomal exit tunnel is too narrow and the nascent peptide chains cannot form tertiary structures but only local or secondary structures in it. These initial conformations of the proteins in the exit tunnel may influence their subsequent folding process outside the ribosome [4–9] with the details yet to be clarified (see Refs. [10,11]).

Many studies have shown that the ribosome can help protein folding in a particular manner [12–16]. For example, it has been shown that the protein temporarily adopt α-helical structure inside the tunnel [17] The topological network analysis on the ribosome structure based on constraint counting [18] has also showed that the exit tunnel is flexible and expandable at the first half part between the PTC and ribosomal L22 protein (called the *folding zone*) [19]. So the nascent peptide chains possibly begin forming their local structures while they are going through the exit tunnel [20–22].

Many people have previously studied protein folding in restricted space. Unlike the bulk environment, confined environment could greatly reduce the conformation space and form a special framework folding pathway [23]. Pande and coworkers have showed that confined proteins in solvent environment facilitates their forming into the native state [24]. Tian and Garcia have built a 20-Å radius fullerene ball to confine the motion of a miniprotein Trp cage and found that the hydrophobic interior surface of the ball could stabilize the folded structure [25]. All-atom simulation of a modeled 10-alanine oligopeptide in a translocon tunnel has also given evidence that a short peptide could fold inside an irregular tunnel with a radius varying from 0 Å to 16 Å [26] Moreover, by using a Go-like model, confinement has also been found to be critical for protein folding [27] and dimerization [28] *in vivo*. Although such space confinement differs from that in the ribosomal exit tunnel, it already indicates that the confinement can help the folding of proteins.

Recently, with the coarse-grained model [29] and the Gaussian statistical model [30], it was shown that the α-helix structure could be entropically stabilized in a tunnel with a large-enough diameter, as does the β-hairpin [31]. To directly study this problem at the all-atom level for real proteins, in this paper we use all-atom molecular dynamics (MD) to study the local or secondary structure formations of the protein villin headpiece subdomain HP35 in the exit tunnel and their influences on the subsequent folding process outside the ribosome.

II. MATERIALS AND METHODS

We select the protein villin headpiece subdomain HP35 (PDB id: 1yrf) as our model since it has been well studied *in vitro* [32,33]. HP35 is in a three-helix conformation with Helix II (residue 11 to 21) and Helix III (residue 22 to 35) forming a plane and Helix I (residue 1 to 10) perpendicular to the plane (Fig. 1).

To simulate protein folding behavior in the exit tunnel, we, first, build a straight β-sheet structure for HP35 according to its sequence. Its principal axis of inertia then is computed and aligned to the x axis of the Cartesian coordinate system, which enables the protein to extend in the x axis direction. Thus, we can easily construct a cylinder tunnel along the x axis and confine the protein within it. The cylinder tunnel has a radius of 9.0 Å or a width of 18 Å, which imitates the ribosomal exit tunnel with the maximum width of about 20 Å. The length of the tunnel for HP35 is 129.35 Å. This results in 5 Å additional space for the protein in the extended conformation. The cylinder-like tunnel has a rigid and smooth boundary (wall). When the atom hits the wall, it will undergo an elastic collision. To be specific, the velocity along the radial direction is reversed and the tangential component remains unchanged.

We simulate the folding of HP35 in the tunnel at room temperature (298 K) for 20 ns, starting from an extended β-strand conformation. The simulation time in the tunnel is set as 20 ns because the conformations of the protein have no evident changes after 20 ns. The protein then is released into free space to fold freely for another 130 ns. As a

*Corresponding author: yxiao@mail.hust.edu.cn

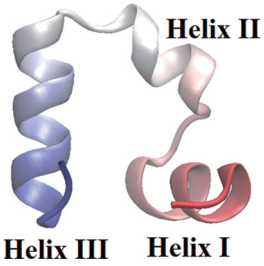

FIG. 1. (Color online) Tertiary structure of the protein villin headpiece subdomain HP35 (PDB id: 1yrf). Helixes I and II are the N-terminus and Helix III is the C-terminus. The picture is created by VMD [34].

comparison, we also conduct 150-ns-long folding simulations at room temperature for HP35 directly in free space, starting from the same extended β-strand conformation. We run eight independent trajectories for each type of simulation with randomly chosen initial atom velocities.

All the simulations are carried out in GB/SA implicit solvent (igb1 in AMBER software) [35] with the AMBER FF03 force field [36]. Lei and Duan [32,33] have shown that such a force field and solvent model can successfully simulate the folding of HP35 into its native structure with accuracy of subangstroms. Langevin dynamics [37] is applied to control the temperature at 298 K. The time step is 1.0 fs. No degrees of freedom are constrained. Recent works of our group showed that such a strategy is proper for peptide folding [38,39]. We wrote the code for the tunnel confinement in FORTRAN and inserted it into the AMBER 9 program as a supplemental subroutine [40].

III. RESULTS AND DISCUSSIONS

To study the role of ribosomal exit tunnel on the protein folding, we, first, put the protein HP35 into a cylinder tunnel and did a molecular dynamics simulation for 20 ns at room temperature (298 K). As a comparison, we also simulated the protein under the same condition but without the tunnel. Figure 2 shows the probabilities that each of the residues in the protein HP35 stays in the helical state during the 20-ns simulation. Here the helical state is determined by

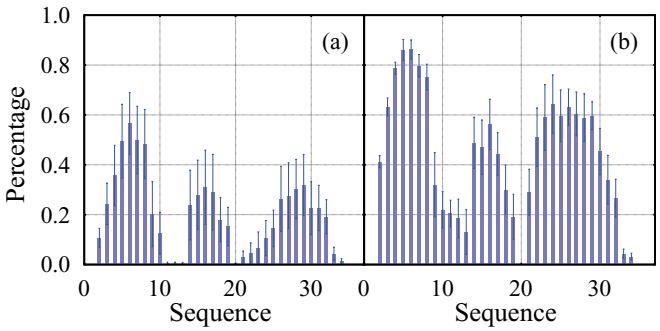

FIG. 2. (Color online) The probability of each residue in the protein HP35 staying in the helical state during 20-ns simulations. Here the helical state is determined by use of DSSP software [41], and the error bars are based on the statistical data of eight independent trajectories. Panels (a) and (b) show simulation results in free space and in the exit tunnel, respectively.

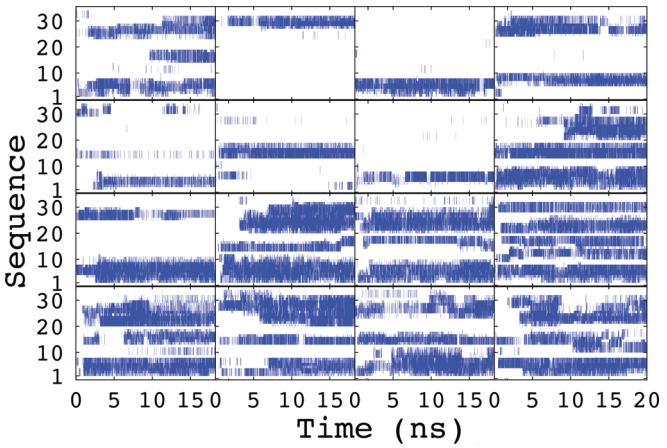

FIG. 3. (Color online) α-helix structure formation of the protein HP35 versus time during 20-ns implicit solvent simulations. Eight subplots at the upper side show eight folding trajectories in free space while eight subplots at the lower are for eight folding trajectories in the exit tunnel. Here the residues in the α-helical state (determined by use of DSSP software [41]) are in blue (dark gray).

DSSP software [41] and then normalized over the time period. Figures 2(a) and 2(b) give the simulation results in free space and the tunnel, respectively. They show that HP35 can form their native helical structure more easily in the tunnel than in the free space, especially for Helix I and Helix III. The formed helical structures also keep stable during the folding in the tunnel. This supports previous suggestions that the ribosomal exit tunnel can help the formations of the helical structures of proteins [20–22].

In Fig. 3, we give detailed information for secondary structure formation in and out of the tunnel. The eight subplots at the top are the data for eight independent simulations in free space, 20 ns for each. The data from the simulations in the tunnel are shown in the eight subplots at the bottom. The regions marked in blue represent the helical conformation. It is clear that in the tunnel the peptide forms helixes very easily and quickly, while in free space it does not. At about 8 ns, all the native helixes have been formed. This fast folding process could be explained by the local interactions in the sequence. In the tunnel the protein cannot form a tertiary structure, so the residues in the protein have chances to form hydrogen bonds with neighboring residues along the chain, which would naturally accelerate the secondary structure formation. Furthermore, the residues in the loops that connect Helix I and Helix II as well as Helix II and Helix III do not fold in most folding trajectories in the tunnel.

In the above, we have showed that the peptide could easily form native secondary structures in the tunnel. Would these local structures remain stable when the peptide moves out from the tunnel into free space? If the secondary structures turned into irregular coils, the role of tunnel on the subsequent folding process is negligible. So in the following we'll test the stability of these secondary structures in further folding in free space. We achieve this by performing further 130-ns simulation starting from the last structure of each of the eight 20-ns simulations in the tunnel. Figure 4 gives the secondary structure formation versus time for HP35 in the whole simulation period. In the first 20 ns the protein is restricted

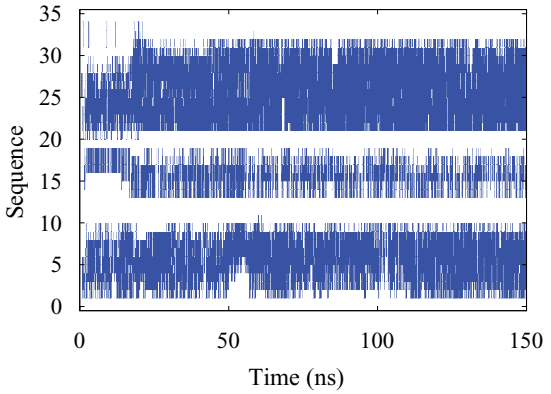

FIG. 4. (Color online) α-helix structure formation of the protein HP35 versus time during a 150-ns simulation. From 0 to 20 ns, the protein is simulated in the tunnel; from 20 to 150 ns, it folds in free space. The residues in the α-helical state (determined by use of DSSP software [41]) are in blue (dark gray).

in the tunnel, and after that the protein is released out of the tunnel and folds in free space. All helixes (Helixes I to III) then form their native secondary structures completely and are in better stability than in the tunnel. In addition, just as we discussed above, there are still no secondary structures found for those residues in the loops between the helixes. In general, the protein well maintains its native secondary structure. The other independent simulations implicate the similar results. As a result, such a large amount of stable secondary structures would certainly improve the formation of tertiary structures.

In the following, we will study how the tunnel confinement affects the formation of tertiary structures. Since the simulation time for each trajectory is only 150 ns, our study focus on the influence of the prefolding on initial stage of free-space folding. Here we use two parameters to describe the tertiary interactions. One is the ratio Q_1 of long-range native contacts in the snapshot structure to those in the native state. Q_1 indicates the completeness of the folding. Another parameter is the ratio Q_2 of long-range non-native contacts to all contacts (including native contacts) in the snapshot structure. Q_2 gives the percentage of wrong interactions in the current structure. The long-range contacts are defined by the C_α-C_α distances between residues being lower than 11 Å and distances along the sequence larger than four residues. The ratios Q_1 and Q_2 for whole protein, Helixes I + II and Helixes II + III, are shown in Fig. 5, respectively. Figure 5 indicates that the prefolding in the tunnel can make the protein forms more native contacts and less non-native ones. Therefore, the tunnel may accelerate the secondary structure formation and reduce the formation of the wrong interactions in the early folding stage, which could accelerate the tertiary structure formation. On the other hand, protein folding in free space is very difficult and the protein tends to form wrong interactions more than correct ones, which may be responsible for the frustrated free-energy landscape. It should be noted that when moving out of the tunnel at 20 ns, the percentage of non-native contacts increases sharply from 20% to 50% [red color curve in Fig. 5(b)]. Since Q_2 for Helix I + II and Helix II + III remain stable [Figs. 5(d) and 5(f)], it means that, after being released from the tunnel, most wrong interactions were formed between Helixes I and III.

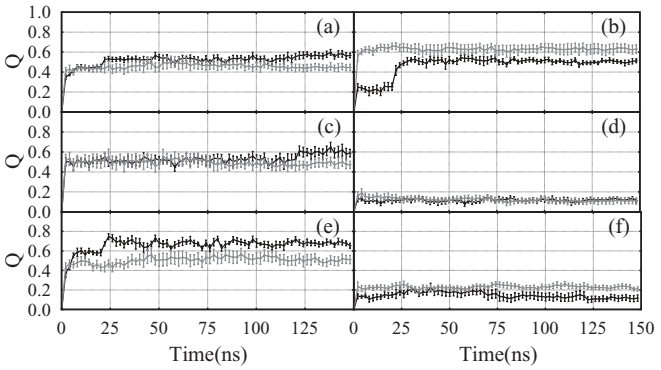

FIG. 5. The ratio Q_1 (left) of long-range native contacts in the snapshot structures to those in the native state and the ratio Q_2 (right) of long-range non-native contacts to all contacts (including native contacts) in the snapshot structures. Panels (a) and (b) show the data for the whole protein, panels (c) and (d) for Helixes I + II, and panels (e) and (f) for Helixes II + III. The black lines denote the data for prefolding in the tunnel (20-ns simulation in the tunnel plus a further 130-ns simulation releasing from the tunnel), and the gray lines denote 150-ns folding without the tunnel. The error bar is based on the statistical data of eight independent trajectories for each case.

We further plot the free-energy landscape for HP35 folding in free space for 130-ns folding starting from the final structures of 20-ns prefolding in the tunnel [Fig. 6(a)] and 150-ns folding starting from an extended beta structure [Fig. 6(b)]. Both combine eight independent trajectories. The order parameters are the RMSD (root-mean-square deviation) values of the N terminus and C terminus relative to the native structure. Here the N terminus is residues 1 to 20, and the C terminus is residues 12 to 35. We find that prefolding in the tunnel will greatly affect its folding behavior and free-energy landscape. Without prefolding in the tunnel, the free-energy landscape of HP35 shows two large stable ensembles [Fig. 6(b)]. The right ensemble is of initial unfolding and the left one is of minor stability, previously found by Lei and Duan [32,33]. In the minor stable ensemble, the RMSD value of the N-terminus of the protein is lower than 1.0 Å and that of the C-terminus remains at about 4.0 Å, i.e., the N-terminus (Helix I + II) has folded into the native conformation successfully,

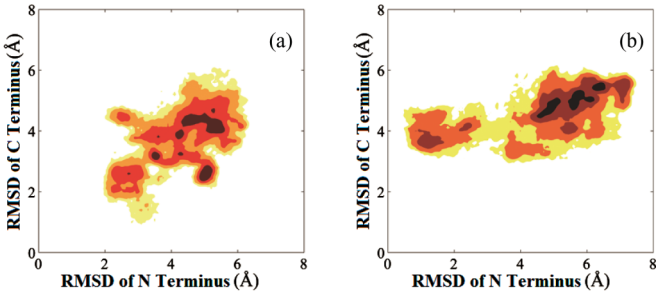

FIG. 6. (Color online) Free-energy landscape of HP35 folding in free space for (a) 130-ns folding starting from the final structures of 20-ns prefolding in the tunnel and (b) 150-ns folding starting from an extended beta structure. The order parameters are RMSD values of the N-terminus and C-terminus relative to the native structure. Here the N-terminus is residues 1 to 20, and the C-terminus is residues 12 to 35. The unit of free energy is kcal/mol.

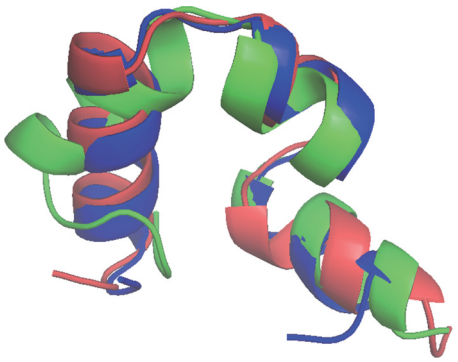

FIG. 7. (Color online) The structure with the smallest RMSD in the folding trajectory with prefolding in the tunnel (red or gray, RMSD 2.1 Å) and direct folding in the free space (green or light gray, RMSD 3.5 Å). For comparison, the native structure is also shown in the figure (blue or dark gray).

while its C-terminus (Helix II + III) still stays in unfolded states. Lei and Duan [32,33] have shown that this minor stable ensemble is from the folding pathway of HP35. Therefore, the high probability for HP35 to trap into this minor stable state will greatly delay its folding process and decrease sampling efficiency. However, if HP35 folds first in the tunnel and then in the free space, both N- and C-termina will fold simultaneously to 2.0 Å, thus avoiding the off-pathway minor states. The minimum RMSD in this case reaches 2.1 Å, which indicates the structure is close to the native one (Fig. 7). These results show that the tunnel may affect the folding pathway of HP35 and make it fold more efficiently. However, this needs further study.

In the following, we study the motion of the protein in the folding process. For this purpose, principal component analysis (PCA) [42] is a good tool. Here, as an illustration, we show PCA results of typical trajectories with and without prefolding in the exit tunnel. All the snapshots in the trajectory are projected onto a 2D space spanned by the first two principal axes (Fig. 8). Each point in the figure is one snapshot of the trajectory and its color shows the simulation time. From Fig. 8, it is clear that both trajectories show two clusters. For the folding trajectory with prefolding in the exit tunnel, the small cluster at right corresponds to the initial folding stage in the tunnel (20 ns) and the large cluster at left represents the second folding stage out of the tunnel (130 ns) [Fig. 8(a)], whereas for

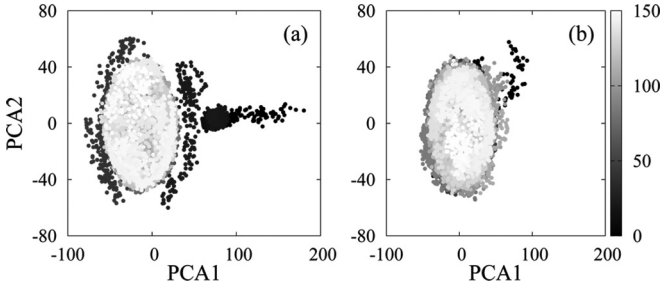

FIG. 8. Principal component analysis for typical folding trajectories (totally 150 ns) with (a) prefolding in the exit tunnel and (b) direct folding in the free space. All the snapshots are projected onto the 2D space spanned by the first two principal axes. The bar on the right indicates the simulation time (in unit of ns).

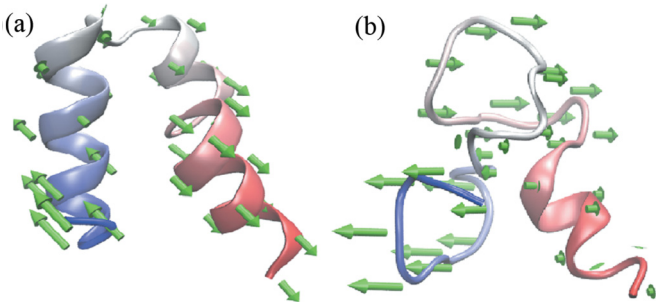

FIG. 9. (Color online) The motion of C_α atoms in HP35 along the direction of the first principal axis in the principal component analysis (shown by arrows) for (a) the folding trajectory with prefolding in the exit tunnel and (b) the direct folding trajectory in free space. The lengths of the arrows represent the motion amplitude. The structure is the snapshot at the center of the folding cluster (shown in Fig. 8).

the folding trajectory in the free space, the small cluster refers to the initial collapsing stage and the large cluster represents the collapsed globular state [Fig. 8(b)]. The small cluster in the folding trajectory with prefolding in the exit tunnel [Fig. 8(a)] is larger than that in the free folding trajectory [Fig. 8(b)] due to the confinement effect. It indicates that the molecule stays in the extended state for a longer time. Moreover, when the protein is released from the tunnel, the second folding cluster is still larger. Because of rich secondary structures, the molecule collapses slowly and samples more boundary points of the cluster. This allows the protein to adjust its conformation in a wide range and help it find the right way to the native state. On the contrary, the free folding trajectory quickly reaches a compact folding cluster. This makes the protein difficult to adjust its conformations.

To give the information about behaviors of the largest motion during the folding, we extract the central snapshot of the large cluster and plot the motion mode of C_α atoms in HP35 along the first principal axis (Fig. 9). The arrows in the snapshot give the directions of the motion and their lengths indicate amplitudes of the motion. For the case with prefolding in the exit tunnel [Fig. 9(a)], the largest PCA mode of the snapshot shows that the most important motion is the separation between two parts of the protein, Helix I and Helix III, while Helix II acts as a hinge and moves much slower than the other two helixes, i.e., the main motion of the protein is adjusting the relative position of Helixes I and III in order to fold into the native structure. As a comparison, the largest PCA mode of the central snapshot in the free folding trajectory shows random directions and magnitudes of motion. Thus, the protein can hardly complete any global domain movement that is critical for it to escape from the local minimum states.

Finally, we discuss the effects of the solvent model on the simulation results. We have used implicit solvent model [35] in all calculations above, which is an approximation to the explicit solvent. Previous studies have shown its reliability in protein folding [32,33,38] and binding free energy calculation [43]. Here, to further compare the implicit and explicit solvent model, we also perform primary simulations in explicit solvent. The molecule also starts from an extended conformation but immerged into a 135.42 Å × 38.73 Å × 34.23 Å box with 11889 TIP3P waters [44]. Just as in the implicit solvent model,

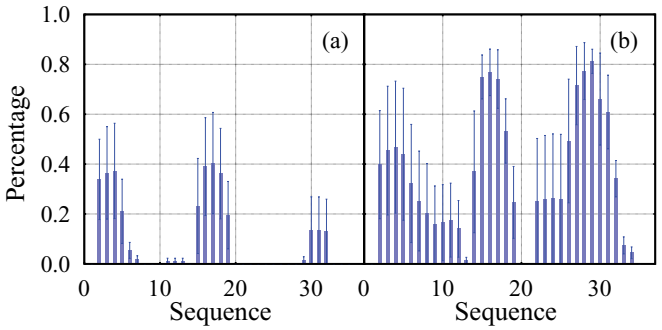

FIG. 10. (Color online) The probability of each residue in the protein HP35 staying in the helical state during 100-ns explicit solvent simulations. Here the helical state is determined by use of DSSP software [41] and the error bars are based on statistical data of three independent trajectories. Panels (a) and (b) show the simulation results in free space and in the exit tunnel, respectively.

two kinds of simulations are carried out. In the first kind of simulation, the HP35 folds directly in the explicit solvent for 100 ns. In the second kind of simulation, it folds within the tunnel for 100 ns. Here, when the molecule is in the tunnel, in order to take the tunnel effect and the periodicity of the system into account simultaneously, the tunnel condition is used only to constrain the HP35 but not the water molecules. The results of the simulations are given in Fig. 10. Similarly to Fig. 2, it shows the probabilities of each residue in the protein HP35 staying in the helical state during the 100-ns simulation; Fig. 10(a) shows folding directly in free space and Fig. 10(b) shows folding in the tunnel. The results are the same as those in the implicit solvent, i.e., HP35 is more apt to be in the native helical structure in the tunnel compared with that in free space.

To check the stability of the secondary structure in explicit solvent, we select one trajectory in the exit tunnel and extend the simulation to 200 ns. The secondary structure formation versus time is shown in Fig. 11. Similarly to the simulation in implicit solvent, all helixes (Helixes I to III) fold into their native helical states in explicit solvent, and these secondary structures remain stable. Such favorable secondary structures

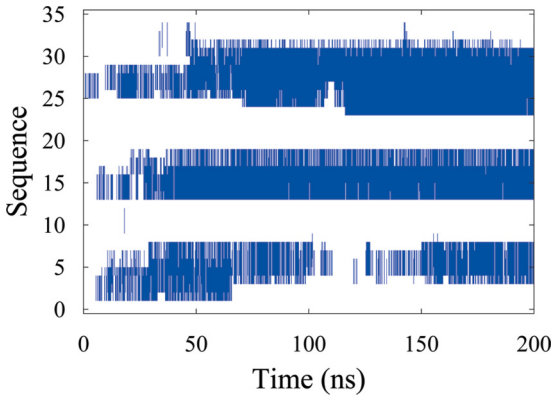

FIG. 11. (Color online) α-helix structure formation of the protein HP35 versus time in the explicit solvent. For the first 100 ns, the protein is simulated in the tunnel, and for the last 100 ns, it is released to free space. The residues in the α-helical state (determined by use of DSSP software [41]) are in blue (dark gray).

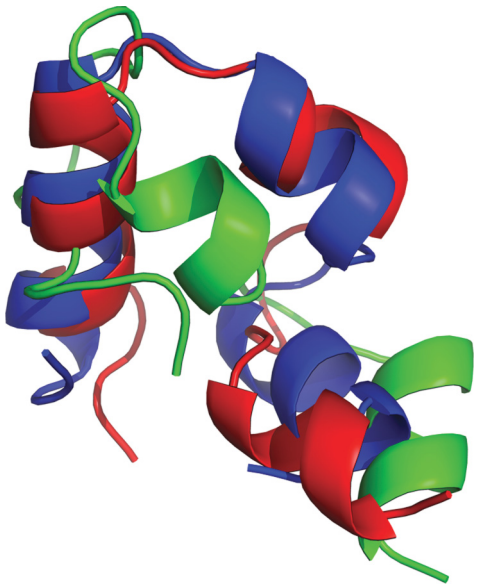

FIG. 12. (Color online) The structure with the smallest RMSD in the folding trajectory with prefolding in the tunnel (red or gray, RMSD 3.2 Å) and direct folding in the free space (green or light gray, RMSD 6.7 Å). For comparison, the native structure is also shown in the figure (blue or dark gray).

seem to make it fold into to the native state more easily than folding directly in the free space (Fig. 12). However, the loops between helixes are a little longer than in the implicit solvent. This indicates that the formation of helical structures requires longer times in explicit solvent. Therefore, long-time simulations with sufficient quantity are desirable to further validate the effects of the solvent on succeeding folding after releasing from the exit tunnel.

IV. CONCLUSION

The famous *Anfinsen*'s experiment indicates that the correct folding of proteins is determined not only by internal interactions but also their external interactions with the environment, such as with solvent, chaperon, and ribosomes [45] The external environment affects the folding pathway and efficiency. One effect, due to the ribosome in the protein folding, is its narrow and long space constraint in the exit tunnel. With such a constraint, protein is thought to undergo a cotranslational folding process [23]. In this paper we studied the folding behavior of the protein HP35 in the tunnel by molecular simulation with all-atom model. It was found that HP35 has a strong tendency to form correct secondary or local structures in the exit tunnel. This prefolding structure may serve as a good starting point for the subsequent free folding outside the ribosome and channels the protein to form the native contact. Our results reveal the possible function of ribosome in the protein folding process and provide a potential way to explain the fast folding mechanism of proteins *in vivo*.

ACKNOWLEDGMENTS

We are grateful for valuable discussions with Yong Duan. This work is supported by the NSFC under Grants No. 11074084 and No. 11174093.

[1] J. Harms, F. Schluenzen, R. Zarivach *et al.*, Cell **107**, 679 (2001).
[2] W. J. Netzer and F. U. Hartl, Nature **388**, 343 (1997).
[3] J. F. Zhuo, L. S. Zhang, C. J. Chen *et al.*, Int. J. Mod. Phys. B **18**, 2195 (2004).
[4] P. M. Petrone, C. D. Snow, D. Lucent *et al.*, Proc. Natl. Acad. Sci. USA **105**, 16549 (2008).
[5] J. H. Peterson, C. A. Woolhead, and H. D. Bernstein, Mol. Microbiol. **78**, 203 (2010).
[6] C. M. Kaiser, D. H. Goldman, J. D. Chodera *et al.*, Science **334**, 1723 (2011).
[7] I. C. Agmon, FASEB J. **26**, 2277 (2012).
[8] J. Lu, W. R. Kobertz, and C. Deutsch, J. Mol. Biol. **371**, 1378 (2007).
[9] J. Lu and C. Deutsch, J. Mol. Biol. **384**, 73 (2008).
[10] L. D. Cabrita, C. M. Dobson, and J. Christodoulou, Curr. Opin. Struct. Biol. **20**, 33 (2010).
[11] D. V. Fedyukina and S. Cavagnero, Annu. Rev. Biophys. **40**, 337 (2011).
[12] S. Chattopadhyay, S. Pal, D. Pal *et al.*, Biochim. Biophys. Acta. **11**, 293 (1999).
[13] S. A. Etchells and F. U. Hartl, Nat. Struct. Mol. Biol. **11**, 391 (2004).
[14] M. S. Svetlov, V. A. Kolb, and A. S. Spirin, Mol. Biol. **41**, 96 (2007).
[15] D. Samanta, D. Mukhopadhyay, S. Chowdhury *et al.*, J. Bacteriol. **190**, 3344 (2008).
[16] D. Das, A. Das, D. Samanta *et al.*, Biotechnol. J. **3**, 999 (2008).
[17] C. A. Woolhead, P. J. McCormick, and A. E. Johnson, Cell **116**, 725 (2004).
[18] S. Fulle and H. Gohlke, J. Mol. Biol. **387**, 502 (2009).
[19] J. Lu and C. Deutsch, Nat. Struct. Mol. Biol. **12**, 1123 (2005).
[20] R. J. Gilbert, P. Fucini, S. Connell *et al.*, Mol. Cell. **14**, 57 (2004).
[21] X. F. Xu and D. P. Cao, Eur. Phys. J. E **32**, 307 (2010).
[22] L. W. Tu and C. Deutsch, J. Mol. Biol. **396**, 1346 (2010).
[23] W. Lee, X. Zeng, H. X. Zhou *et al.*, J. Biol. Chem. **285**, 38167 (2010).
[24] D. Lucent, V. Vishal, and V. S. Pande, Proc. Natl. Acad. Sci. USA **104**, 10430 (2007).
[25] J. Tian and A. E. Garcia, J. Am. Chem. Soc. **133**, 15157 (2011).
[26] J. Gumbart, C. Chipot, and K. Schulten, J. Am. Chem. Soc. **133**, 7602 (2011).
[27] J. Mittal and R. B. Best, Proc. Natl. Acad. Sci. USA **105**, 20233 (2008).
[28] W. Wang, W. X. Xu, Y. Levy *et al.*, Proc. Natl. Acad. Sci. USA **106**, 5517 (2009).
[29] G. Ziv, G. Haran, and D. Thirumalai, Proc. Natl. Acad. Sci. USA **102**, 18956 (2005).
[30] H. X. Zhou, Arch. Biochem. Biophys. **469**, 76 (2008).
[31] S. Kirmizialtin, V. Ganesan, and D. E. Makarov, J. Chem. Phys. **121**, 10268 (2004).
[32] H. X. Lei and Y. Duan, J. Mol. Biol. **370**, 196 (2007).
[33] H. X. Lei, C. Wu, H. G. Liu *et al.*, Proc. Natl. Acad. Sci. USA **104**, 4925 (2007).
[34] W. Humphrey, A. Dalke, and K. Schulten, J. Mol. Graphics **14**, 33 (1996).
[35] D. Qiu, P. S. Shenkin, F. P. Hollinger *et al.*, J. Phys. Chem. A **101**, 3005 (1997).
[36] Y. Duan, C. Wu, S. Chowdhury *et al.*, J. Comput. Chem. **24**, 1999 (2003).
[37] R. W. Pastor, B. R. Brooks, and A. Szabo, Mol. Phys. **65**, 1409 (1988).
[38] C. Chen and Y. Xiao, Bioinformatics **24**, 659 (2008).
[39] Y. Xiao, C. Chen, and Y. He, Int. J. Mol. Sci. **10**, 2838 (2009).
[40] D. A. Case, T. E. Cheatham III, T. Darden *et al.*, J. Comput. Chem. **26**, 1668 (2005).
[41] W. Kabsch and C. Sander, Biopolymers **22**, 2577 (1983).
[42] N. Elmaci and R. S. Berry, J. Chem. Phys. **110**, 10606 (1999).
[43] M. Lapelosa, E. Gallicchio, and R. M. Levy, J. Chem. Theory Comput. **8**, 47 (2012).
[44] W. L. Jorgensen, J. Chandrasekhar, J. D. Madura *et al.*, J. Chem. Phys. **79**, 926 (1983).
[45] C. B. Anfinsen, Science **181**, 223 (1973).